Downloaded from rsta.royalsocietypublishing.org

PHILOSOPHICAL TRANSACTIONS OF THE ROYAL SOCIETY A MATHEMATICAL, PHYSICAL & ENGINEERING SCIENCES

Rotation and the Internal Structures of the Major Planets and their Inner Satellites [and Discussion]

S. F. Dermott and A. H. Jupp

Phil. Trans. R. Soc. Lond. A 1984 **313**, 123-139
doi: 10.1098/rsta.1984.0088

Email alerting service

Receive free email alerts when new articles cite this article - sign up in the box at the top right-hand corner of the article or click **here**

To subscribe to *Phil. Trans. R. Soc. Lond. A* go to: **http://rsta.royalsocietypublishing.org/subscriptions**

This journal is © 1984 The Royal Society

Downloaded from rsta.royalsocietypublishing.org

Phil. Trans. R. Soc. Lond. A **313**, 123–139 (1984) [123]
Printed in Great Britain

Rotation and the internal structures of the major planets and their inner satellites

By S. F. Dermott

Center for Radiophysics and Space Research, Cornell University, Ithaca, New York 14853-0355, *U.S.A.*

Measurements of the rotational periods coupled with those of the masses, the mean radii and the shapes or the gravitational moments (J_2 and J_4) enable important constraints to be placed on the internal structures of some remote bodies. Values of J_2 for Uranus and Neptune have been calculated from the observed precession rates of the narrow eccentric and inclined Uranian rings and of the orbit of Triton, Neptune's massive satellite. Recent observations of the motions of spots have yielded reliable rotational periods for these planets. These observations are used to show that Uranus and Neptune may have quite different internal structures. The shapes of satellites that are close to their primaries may yield information on the degree of internal differentiation of these bodies. Io, Mimas, Enceladus and Miranda are of interest in this respect. Residuals in the observed precession rates of the Uranian rings, *ca.* 0.005°/day, that cannot be accounted for by the best-fit model of J_2 and J_4 may be related directly to observed irregular variations in ring width of magnitude over 2 km and may indicate the existence of shepherding satellites with mass ratios of over 10^{-10}. If this is the case, then the effects of these satellites on the precession rates of the rings will result in an appreciable uncertainty in the value of J_4 for Uranus.

1. Introduction

The external gravitational field of a non-rotating planet in hydrostatic equilibrium would give no clue as to the nature of its internal structure. However, slow rotation of such a body produces an axially symmetric distortion and the magnitude of the equatorial bulge is determined by both the magnitude of the disturbing potential and the internal density distribution. The observables are the rotational period T, the mean density $\langle\rho\rangle$, the oblateness, $f = 1 - R_p/R_r$ (where R_p and R_r are the polar and equatorial radii), and the coefficients $J_2, J_4, \ldots$ in the harmonic expansion of the external potential. The magnitude of the disturbing potential in this problem is determined by the ratio q of the centrifugal and the gravitational equatorial accelerations. $q = 3\Omega^2/4\pi G\langle\rho\rangle$, where Ω is the rotational frequency and G is the gravitational constant. The oblateness f of some equipotential surface (exterior to the planet) of equatorial radius R_r that rotates as a whole at some frequency Ω and the coefficient J_2 in the harmonic expansion of the gravitational potential external to that surface are related (to first order in small quantities) by

$$2f = 3J_2 + q, \tag{1}$$

where $\langle\rho\rangle$ is the mean density of the material interior to the surface and R_r is the normalizing radius in the expansion of the potential. In applying this equation, one should be aware that the rotational frequency of the surface and that of the 'solid' body of the planet may be different

The Royal Society is collaborating with JSTOR to digitize, preserve, and extend access to *Philosophical Transactions of the Royal Society of London. Series A, Mathematical and Physical Sciences.* www.jstor.org

Downloaded from rsta.royalsocietypublishing.org

and that R_r may not be equal to the equatorial radius of the planet R_e, which, for modelling purposes, is usually taken to be the surface at which the pressure is 1 bar (Hubbard 1984)†.

In this paper, we are chiefly concerned with the internal structures of Uranus and Neptune. For these planets, since $q \ll 1$ (see table 1), J_2 and f increase linearly with q. Hence, the ratio J_2/f is independent of q and only depends on the internal density distribution. The Darwin–Radau relation makes the stronger statement that J_2/f depends only on the moment of inertia factor C ($= I/MR^2$, where I is the moment of inertia and M is the mass of the planet). In fact, J_2/f only places an upper bound on C. The point-core model, in which the mean density and the moment of inertia factor are reproduced by a model planet with a mantle of uniform density and a massive point-core, places a lower bound on C. We use these bounds to compare the internal density distributions of the major planets.

Other topics discussed in this paper include the influence of putative shepherding satellites on the precession rates of the Uranian rings and the effect that these satellites may have on the determination of J_2 and J_4. We also use our bounds on the moment of inertia factor C to place bounds on the shapes of the satellites Io, Mimas, Enceladus and Miranda. Voyager observations of the shapes of Io and Mimas are now available (Davies 1983; Davies & Katayama 1983) and it would appear that the mean shapes are too spherical to be accounted for by any reasonable density distributions.

2. The Darwin–Radau relation

The bounds that can be placed on the moment of inertia factor are best illustrated by a specific example. The oblateness f and the gravitational moment J_2 of a model planet in hydrostatic equilibrium with a uniform core of density ρ and radius r and a uniform mantle of density σ and outer radius unity are given by

$$f = \tfrac{5}{4}Hq, \tag{2}$$

$$J_2 = \tfrac{5}{6}(H - \tfrac{2}{5})\, q, \tag{3}$$

in which the dimensionless constants are

$$H = \frac{\frac{2}{5}(\langle\rho\rangle/\rho)\,[1+\frac{3}{5}(\delta/\gamma)\,r^2]}{\frac{2}{5}(\sigma/\rho)+\delta-\frac{9}{25}(\delta/\gamma)\,(\sigma/\rho)\,r^2}, \tag{4}$$

$$\delta = (1-\sigma/\rho)\,r^3 \tag{5}$$

and

$$\gamma = \tfrac{2}{5}+\tfrac{3}{5}\sigma/\rho \tag{6}$$

(Dermott 1979*a*, *b*). (For a planet of uniform density in hydrostatic equilibrium H is unity.) For this particular model

$$C = \tfrac{2}{5}[\sigma/\langle\rho\rangle + (1-\sigma/\langle\rho\rangle)\,r^2] \tag{7}$$

and

$$\langle\rho\rangle/\rho = \delta + \sigma/\rho. \tag{8}$$

Specifying C and r uniquely determines σ/ρ, H and J_2/f. Plots of J_2/f against C for particular

† 1 bar = 10^5 Pa.

Downloaded from rsta.royalsocietypublishing.org

values of r are shown in figure 1. The bounds on C for a particular value of J_2/f that are found from (2)–(8) by allowing r to tend to zero and unity are

$$C-\tfrac{15}{8}(\tfrac{2}{5}-C)^2 \leqslant J_2/f \leqslant C. \tag{9}$$

The lower bound on J_2/f is equivalent to the Darwin–Radau relation (Darwin 1899) and the upper bound is that given by the point-core model. It can be shown that these bounds apply to any planet in stable, hydrostatic equilibrium. The Darwin–Radau bound follows immediately from the fact that the function $\psi(\eta)$ defined by Radau's equation

$$\psi(\eta) = (1+\tfrac{1}{2}\eta-\tfrac{1}{10}\eta^2)/(1+\eta)^{\frac{1}{2}} \tag{10}$$

has a *maximum* value of 1.00074. In the derivation of the Darwin–Radau relation, $\psi(\eta)$ is set equal to unity (see, for example, Jeffreys 1970). However, for certain planetary models, particularly those for which the moment of inertia factor is low, this is not a good approximation.

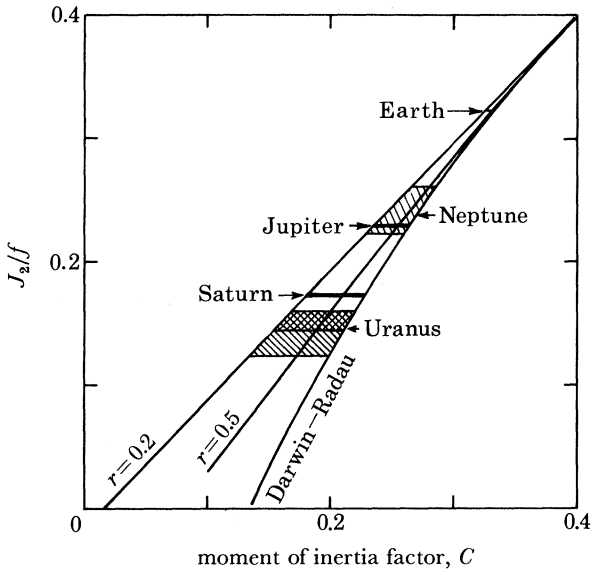

FIGURE 1. Bounds on the moment of inertia factors C can be estimated from the observed values of J_2/f. Independent of any interior model, we can state that Saturn is more centrally condensed than Jupiter and that Uranus is probably the most centrally condensed planet in the Solar System. The oblateness f of Neptune is calculated from J_2, $\langle\rho\rangle$ and T ($=18.2\pm0.4$ h: see table 1), and the same procedure has been followed for Jupiter and Saturn. It would appear that Neptune and Uranus have quite different interiors.

The bounds on C given by (9) allow us to make statements about the internal density distributions of the planets that are independent of models of their interiors. For example, Saturn is less massive than Jupiter and has a considerably lower mean density (see table 1) and yet the observed values of J_2/f (or, in these cases, J_2, T and $\langle\rho\rangle$) indicate that it has a lower moment of inertia factor. Thus, since Saturn is much more centrally condensed than Jupiter, the planets probably have quite different chemical compositions.

It is also useful to note that J_2/f is roughly equal to C. Thus, plots of $\mathrm{d}C/\mathrm{d}R$ and $\mathrm{d}M/\mathrm{d}R$ against R for a model interior indicate those parts of the planet that actually constrain the model through the observables J_2, f, T and $\langle\rho\rangle$. Typical models of Jupiter (Hubbard, personal

Downloaded from rsta.royalsocietypublishing.org

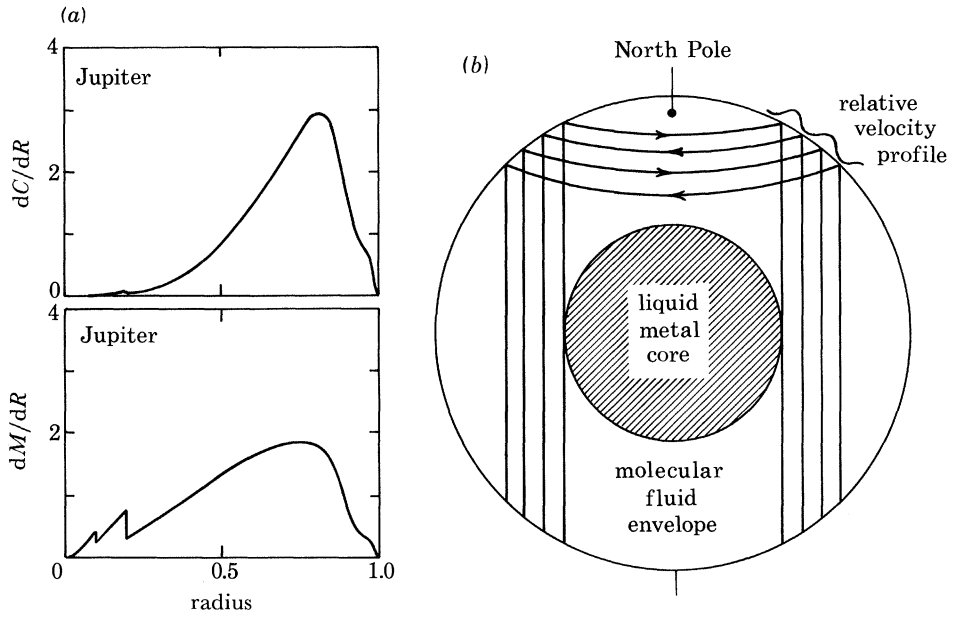

FIGURE 2. The contributions of the outer layers of Jupiter (and Saturn) to the moment of inertia factor C and the mass M are small (*a*). Hence, the differential rotation of the outer layers depicted in (*b*) has only a small effect on J_2 and f.

communication, 1983), for example, are dominated by the contributions from the material at $R \approx 0.8$ (see figure 2). Material with $R < 0.3$ makes a negligible contribution to C and this material could be replaced by a point-core: the structures of the cores of the giant planets cannot be deduced from their observed gravitational moments.

The observed zonal currents in the atmospheres of Jupiter and Saturn are highly symmetric with respect to their equators and this suggests that angular velocity is constant on cylindrical surfaces parallel to their rotation axes (Ingersoll & Pollard 1982): see figure 2. Thus, our implicit assumption of solid body rotation may be violated in the outer layers of these planets. However, even on Saturn, the high velocity zonal currents are confined to latitudes within 20° of the equator and these correspond to $R > 0.94$. Beyond $R = 0.8$ both $\mathrm{d}C/\mathrm{d}R$ and $\mathrm{d}M/\mathrm{d}R$ decrease markedly and material with $R > 0.94$ makes only small contributions to C and M. Hubbard (1982) has shown that the allowances that have to be made for differential rotation are small. For Saturn, $R_\mathrm{e} - R_\mathrm{p} \approx 5000$ km, of which the zonal currents make a contribution *ca.* 50 km. The corresponding figures for Jupiter are 4600 and 6 km, respectively. Moreover, the corrections that have to be made to $J_2, J_4, \ldots$ for modelling purposes can be made in a manner that is largely independent of the model interior. Thus, possible complications due to differential rotation pose only a minor problem to the modelling process. However, the existence of large zonal currents does call into question the true 'solid-body' period of the planet. Allison & Stone (1983) have suggested that the solid-body period of Saturn may be about 1% less than the radio period. By using the Darwin–Radau relation, it can be shown that for Saturn a 1% error in T would be equivalent to a 2.7% error in J_2. Accurate values for the higher gravitational moments J_4 and J_6 are of little use without a correspondingly accurate value of T (Hubbard 1984).

PHILOSOPHICAL TRANSACTIONS OF THE ROYAL SOCIETY A MATHEMATICAL, PHYSICAL & ENGINEERING SCIENCES
PHILOSOPHICAL TRANSACTIONS OF THE ROYAL SOCIETY A MATHEMATICAL, PHYSICAL & ENGINEERING SCIENCES

TABLE 1. ROTATIONAL DATA FOR THE MAJOR PLANETS[1]

	mass[2] (Earth masses)	reference radius, R_r^3 km	mean density, $\langle\rho\rangle^3$ g cm^{-3}	oblateness, f	$10^3 \times J_2$	period, T/h	q
Jupiter	317.777 ± 0.001[4]	71 398	1.332	0.0648 ± 0.0001[8]	14.733 ± 0.004[4]	$9.924\,92 \pm 0.000\,01$[13]	0.083
Saturn	95.165 ± 0.005[5]	60 000	0.689	0.088 ± 0.006[9]	16.479 ± 0.018[5]	10.657 ± 0.002[14]	0.139
Uranus	14.51 ± 0.01[6]	26 200	1.180	0.024 ± 0.003[10]	3.349 ± 0.005[1]	(15.6 ± 1.4)[15]	0.038
Neptune	17.02 ± 0.01[7]	25 225	1.540	(0.0170 ± 0.0010)[11]	4.1 ± 0.3[12]	18.2 ± 0.4[16]	0.021

[1] Based in part on data tabulated by Elliot & Nicholson (1984).

[2] The measured quantity is GM. (These figures assume that $G = 6.670 \times 10^{-8}$ dyn cm^2 g^{-2} and that $M_\odot = 5.977 \times 10^{27}$ g (1 dyn $= 10^{-5}$ N).)

[3] The reference radius R_r is the radius used in the harmonic expansion of the gravitational field. It is the equatorial radius of the equipotential surface for which equation (1) linking J_2, f and T applies. The mean density $\langle\rho\rangle$ tabulated here refers to the mass enclosed by that surface. For modelling purposes the equatorial radius R_e of a surface at a specific pressure is required.

[4] Null (1976).

[5] Null *et al.* (1981).

[6] Dunham (1971).

[7] Gill & Gault (1968).

[8] Lindal *et al.* (1981).

[9] Gehrels *et al.* (1970).

[10] Elliot *et al.* (1981).

[11] Derived from the tabulated values of J_2 and T. (Compare with the observed value of 0.021 ± 0.004 (Kovalesky & Link 1969).)

[12] Calculated by using the analysis of Harris (1984), the Darwin–Radau relation and the tabulated value of T assuming that the mass ratio m/M of Triton and Neptune is $0.001\,28 \pm 0.000\,23$ (Alden 1943).

[13] Smoluchowski (1976).

[14] Desch & Kaiser (1981).

[15] Calculated by Elliot & Nicholson (1984) from the observed values of J_2 and T. Observed values of T have a weighted mean of 16.31 ± 0.27 h (Goody 1982) and direct observations of the motions of individual spots give periods of 16.0, 16.2, and 16.4 h (O'Meara 1984).

[16] Belton & Terrile (1984).

Downloaded from rsta.royalsocietypublishing.org

Downloaded from rsta.royalsocietypublishing.org

3. Uranus

For the purposes of this discussion, the uncertainties in the mean densities of Uranus and Neptune can be neglected. In using J_2/f to compare the moment of inertia factors, therefore, one has to choose between using the observed value of f or the value derived from the observed values of J_2 and T through (1).

J_2 for Uranus is now known with great precision from observations of the precession rates of the narrow eccentric and inclined rings (Elliot & Nicholson 1984). The putative shepherding satellites have a negligible effect on the determination of J_2 but this may not be the case for J_4 (see §5). Since the rotational period of Uranus is still uncertain, the observed value of f is probably the most useful parameter. Analysis of Stratoscope II images of Uranus yields $f = 0.022 \pm 0.001$ (Franklin *et al.* 1980), hence $J_2/f = 0.153 \pm 0.008$ (the cross-hatched area in figure 1). This value of f has a useful precision and refers to a region near the cloud deck, however, the analysis assumes that there is no latitude-dependent limb darkening (French 1984). Stellar occultation observations yield $f = 0.024 \pm 0.003$ (Elliot *et al.* 1981) and $J_2/f = 0.142 \pm 0.018$ (the hatched *and* cross-hatched area in figure 1). This value of f is unaffected by limb-darkening but refers to a level at a pressure *ca.* 1 μbar at a height *ca.* 500 km above the clouds. If there are significant meridional temperature gradients in the region between these atmospheric levels, then the oblateness could vary substantially with height, as was found by French & Taylor (1981) for Mars (French 1984). Furthermore, French (1984) points out that the half-light points used in the occultation method lie on a surface, which may differ substantially from an equipotential surface, particularly if, like Uranus, the atmosphere has strong vertical temperature variations (French *et al.* 1983).

Despite these problems, we note that the two independent methods of measuring f give consistent values. The value $f = 0.024 \pm 0.003$ implies a rotational period of 15.6 ± 1.4 h (Elliot & Nicholson 1984) and this is consistent with the weighted mean of the observed periods (16.31 ± 0.27 h) quoted by Goody (1982). More importantly, O'Meara (1984) has recently reported observations of the motions of spots on Uranus and these give periods of 16.0, 16.2 and 16.4 h. These variations presumably indicate the existence of moderately strong zonal currents. This level of consistency suggests that we can be reasonably confident that J_2/f for Uranus is close to 0.15.

For $J_2/f \approx 0.15$, the bounds on C given by (9) and figure 1 are not particularly useful. However, consideration of the possible equations of state imposes tighter bounds and I have found that existing planetary models (Hubbard, personal communication) plot in the region between the $r = 0.5$ and the Darwin–Radau lines. For the uniform core–uniform mantle discussed in this paper, if $r = 0.5$, then for $C < 0.2$ we must have $\sigma/\rho < \frac{1}{17}$. This very high density contrast implies that values of J_2/f corresponding to $C \lesssim 0.2$ and $r < 0.5$ should be regarded as highly unlikely. Hence, from figure 1, it can be deduced that $C = 0.20 \pm 0.03$ and that Uranus is probably the most centrally condensed planet in the Solar System.

4. Neptune

The precession rate of Triton's inclined orbit has been rediscussed by Harris (1984) in a major new analysis of all the available photographic observations. The analysis is complicated (or made more interesting) by the fact that the orbital angular momentum of Triton is not

Downloaded from rsta.royalsocietypublishing.org

negligible compared with the spin angular momentum of Neptune. J_2 is given by

$$J_2 = \frac{4}{3}\left(\frac{a}{R_r}\right)^2 \frac{T_0}{\sin 2(i+\epsilon)} \frac{\sin i}{T_p}, \tag{11}$$

where i is the inclination of Triton's orbit to the invariable plane, ϵ is the angle between Neptune's spin axis and the pole of the invariable plane, T_0 is Triton's orbital period, T_p is the nodal precession period and a is the semimajor axis or radius of Triton's circular orbit. Since the components in the invariable plane of the orbital angular momentum of Triton and the spin angular momentum of Neptune are equal and opposite, we have

$$\sin \epsilon = \frac{n}{C\Omega}\left(\frac{a}{R_e}\right)^2 \frac{m}{M} \sin i, \tag{12}$$

where m/M is the mass ratio of Triton and Neptune and n is Triton's mean motion. Since the spin of Neptune Ω is prograde, whereas Triton's orbit is retrograde (Belton & Terrile 1984), n and Ω have opposite signs and the coefficient in (12) is negative.

The only appreciable uncertainties in (11) are those associated with the angles i and ϵ. Harris's analysis of the photographic observations, which span 13% of the precession period, yields

$$i = 21.0° \pm 1.5°. \tag{13}$$

Alden (1943) obtained the mass ratio

$$m/M = 0.00128 \pm 0.00023 \tag{14}$$

from observations of the barycentric motion of Neptune against the background stars.

Measurements of Neptune's rotational period have recently been reviewed by Belton & Terrile (1984). Techniques for extracting periodicities from extended time-series of photometric observations yield a number of precise periods in the range 17.71 to 18.56 hours (Slavsky & Smith 1978; Brown *et al.* 1981; Belton *et al.* 1981). Recent observations of the motions of the spotlike markings seen on Neptune when the planet is imaged in a narrow range of wavelengths centred on the 8900 Å† methane absorption band (Smith *et al.* 1979) leave no doubt that these periodicities represent true atmospheric rotational periods. The bright spots have been tracked over 7 Neptune rotations and yield an atmospheric rotation period of 17.83 ± 0.1 h (Terrile *et al.* 1984). Belton & Terrile (1984) conclude that zonal currents exist on Neptune with velocity contrasts of at least 109 m s^{-1} and that the 'solid-body' period of the planet is probably 18.2 ± 0.4 h.

J_2 for Neptune can be obtained from Harris's analysis through (11) and (12), but only if we have estimates of C and Ω. If we assume that C is given by the Darwin–Radau relation and adopt Belton & Terrile's range of periods, then (1), (9), (11)–(14) can be solved to give the following self-consistent range of values:

$$\begin{aligned} \epsilon &= -2.5° \pm 0.7°; \\ i+\epsilon &= 18.6° \pm 1.8°; \\ J_2 &= 0.0041 \pm 0.0003; \\ f &= 0.0170 \pm 0.0010; \\ J_2/f &= 0.24 \pm 0.02; \\ C &= 0.272 \pm 0.013; \end{aligned}$$

† 1 Å = 10^{-10} m = 0.1 nm.

PHILOSOPHICAL TRANSACTIONS OF THE ROYAL SOCIETY A MATHEMATICAL, PHYSICAL & ENGINEERING SCIENCES

PHILOSOPHICAL TRANSACTIONS OF THE ROYAL SOCIETY A MATHEMATICAL, PHYSICAL & ENGINEERING SCIENCES

Downloaded from rsta.royalsocietypublishing.org

Values of J_2/f for Neptune are shown in the upper hatched region of figure 1. Since the above values of C are high, the Darwin–Radau relation in this case is a good approximation: witness how close the $r = 0.5$ and the Darwin–Radau lines are in figure 1. The above values of f are marginally consistent with the observed value of 0.021 ± 0.004 (Kovalesky & Link 1969). The results of the 1983 occultation of Neptune should give a more precise value, but these have yet to be published.

Harris (1984) has questioned Alden's value for mass ratio m/M. If, to take the extreme case, Triton's mass is negligible and $\epsilon = 0$, then $f = 0.0164 \pm 0.0008$ and J_2/f is reduced to 0.225 ± 0.015. However, this does not affect our main conclusion, namely that if Neptune's rotational period is in the range 18.2 ± 0.4 h, then the moment of inertia factors of Uranus and Neptune are quite different and the planets must have widely different chemical compositions. The differences in J_2/f shown in figure 1 are broadly consistent with a decrease in the H_2–He mass fraction for the major planets with increasing distance from the Sun.

5. Shepherding satellites

The nine Uranian rings are probably confined by a number of 'shepherding' satellites (Goldreich & Tremaine 1979) and these satellites may make appreciable contributions to the observed precession rates (Freedman *et al.* 1983). The pericentre precession rate $\dot{\omega}$ arising from the gravitational field of an oblate planet, can be written as

$$c\dot{\omega} = J_2 - \tfrac{5}{2} J_4 (R_r/a)^2, \tag{15}$$

where

$$c = \frac{2a^{\frac{7}{2}}}{3(GM)^{\frac{1}{2}} R_r^2} \tag{16}$$

and a is the *geometrical* semimajor axis of the best-fitting ellipse traced by the ring particles (Elliot & Nicholson 1984). A plot of $c\dot{\omega}$ against $\frac{5}{2}(R_r/a)^2$ should be a straight line of slope $-J_4$ and intercept J_2. Figure 3 shows such a plot for data from the 1981 M.I.T. Uranian ring model (Elliot *et al.* 1981). The points represent the individually fitted precession rates, whereas the quoted values of J_2 and J_4 were determined from the data set as a whole. Figure 3 not only shows that J_4 was then poorly determined, but also suggests that some of the observed discrepancies may be real, particularly that associated with ring 6 which has a magnitude of 0.011 deg/day (cf. $\dot{\omega}_6 = 2.771$ deg/day).

French *et al.* (1982) have since shown that some of the Uranian rings are not only eccentric but are also inclined to the equatorial plane of the planet. The inclusion of the inclinations in the best-fit model reduces the residuals. However, discrepancies in $\dot{\omega}$, *ca.* 0.005 deg/day, still remain (Elliot & Nicholson 1984; Freedman *et al.* 1983) and it is worth asking if these could be due to small, nearby satellites and how that hypothesis could be tested. Freedman *et al.* (1983) have discussed a number of the effects that small satellites would have on the rings, but I point out here that confirmation of the existence of small satellites could probably be most directly achieved by the detection of irregular ring-width variations, that is, width variations not associated with the regular harmonic variation of ring width with true anomaly.

A small satellite of mass m exerts a tidal torque Γ on a nearby, narrow, near-circular ring.

$$\Gamma = 0.399(Gm/nx^2)^2 m_r, \tag{17}$$

Downloaded from rsta.royalsocietypublishing.org

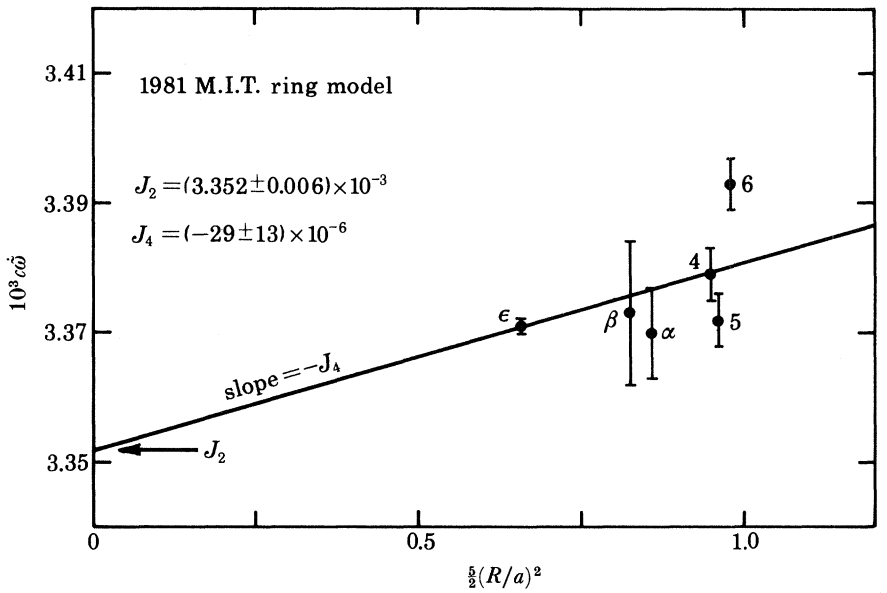

FIGURE 3. The individual precession rates $\dot{\omega}$ are compared with those predicted from the best-fit values of J_2 and J_4 as calculated by Elliot *et al.* (1981). It would appear from these results that the shepherding satellites may make significant contributions to the precession rates.

where x is the mean radial separation of the satellite and the ring, n is the mean motion of the ring particles and m_r is their total mass (Goldreich & Tremaine 1982). Regardless of whether the satellite orbits inside or outside of the ring, the radial gravitational forces that it exerts act to increase the ring's pericentre precession rate by

$$\delta\dot{\omega} = (nm/2\pi M)\,(a/x)^2. \tag{18}$$

The satellite also raises a near-sinusoidal wave on the ring of wavelength

$$\lambda = 3\pi x \tag{19}$$

and amplitude

$$A = 2.24(m/M)\,(a/x)^2\,a \tag{20}$$

(Julian & Toomre 1966; Dermott 1981). Since the net external torque on a ring confined by two satellites and in equilibrium must be zero,

$$m_1/x_1^2 = m_2/x_2^2, \tag{21}$$

where the subscripts refer to the two satellites. It follows that the magnitudes of $\delta\dot{\omega}$ and A associated with each satellite are equal (Dermott 1981). Hence, we can write

$$\delta\dot{\omega}_t = (n/2.24\pi)\,(A/a), \tag{22}$$

where $\delta\dot{\omega}_t$ is the total increase in the precession rate due to both satellites. If $\delta\dot{\omega}_t \approx 0.005$ deg/day, then each satellite raises a wave on the ring of amplitude $A \approx 1.3$ km. These waves can interfere constructively to produce waves of amplitude $2A$ (Dermott 1981). More importantly, if the orbits of the satellites or the ring are eccentric, then $\delta\dot{\omega}_t$ will be largely unchanged but there could be large variations in A. For this reason, equation (22) should be regarded as an approximation.

Downloaded from rsta.royalsocietypublishing.org

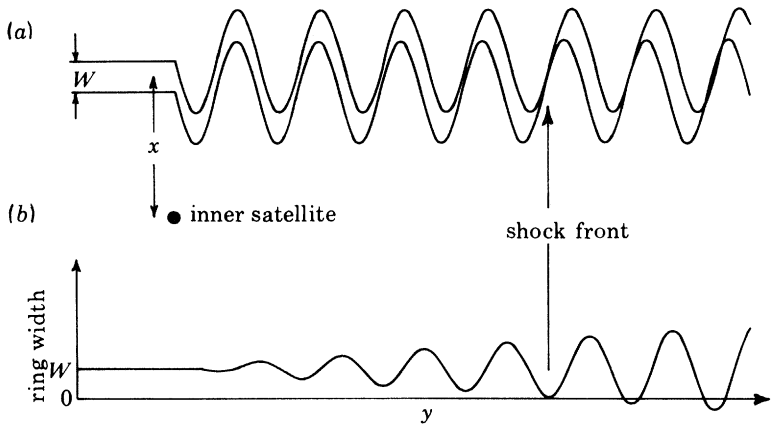

FIGURE 4. A small satellite generates waves of length $3\pi x$, where x is the distance of the satellite from the ring particles. In (*a*) we show the resultant wave pattern in a reference frame rotating with the perturbing satellite. There is a small variation in wavelength across a ring of finite width and this results in a variation in width downstream from the satellite (*b*). (Copyright of the University of Arizona Press.)

For a ring of finite width W, there is a variation of x and wavelength across the ring and this can result in large variations in ring width downstream from the perturbing satellite (Dermott 1984): see figure 3. For most of the Uranian rings it is probable that $W > 2A$, hence the largest variation in width due to one of the satellites is $2A$. It is now well established that the widths of the α- and β-rings of Uranus vary harmonically with true anomaly. The widths of both of these rings increase from a minimum of *ca.* 5 km near pericentre to a maximum of *ca.* 10 km near apocentre (Elliot & Nicholson 1984; P. D. Nicholson & K. Matthews, personal

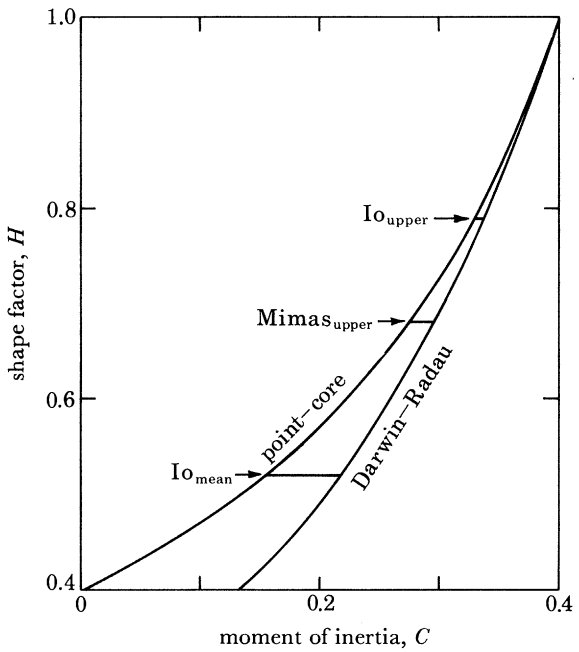

FIGURE 5. For a given shape factor H, the moment of inertia factor C must lie between the upper bound given by the Darwin–Radau relation and the lower bound given by the point-core model. Observed values of H for Io and Mimas are from Davies (1983) and Davies *et al.* (1983), respectively. Only the upper bound on H for Mimas can be shown.

PHILOSOPHICAL TRANSACTIONS OF THE ROYAL SOCIETY A MATHEMATICAL, PHYSICAL & ENGINEERING SCIENCES
PHILOSOPHICAL TRANSACTIONS OF THE ROYAL SOCIETY A MATHEMATICAL, PHYSICAL & ENGINEERING SCIENCES

Downloaded from rsta.royalsocietypublishing.org

TABLE 2. SHAPES OF SATELLITES

satellite	mean density / g cm^{-3}	mean radius / km	q	$b-c$ / km calculated	$a-c$ / km calculated	ratio[1]	$b-c$ / km observed	$a-c$ / km observed	ϕ^2/deg observed
Io[3]	3.56 ± 0.05	1815 ± 5	0.001699 ± 0.00024	3.8	15.7	0.247	0 ± 4	8 ± 4	330 ± 10
Mimas[4]	1.42 ± 0.18[6]	197 ± 3	0.015 ± 0.002	3.4 ± 0.6	16 ± 3	0.210	—	6 ± 3	—
	1.16 ± 0.06[6]	197 ± 3	0.019 ± 0.002	4.2 ± 0.3	20 ± 2	0.208	—	6 ± 3	—
Enceladus[4]	1.27 ± 0.45	251 ± 5	0.008 ± 0.003	2.6 ± 1.1	11 ± 5	0.224	—	8 ± 5	—
Miranda[5]	(1.2)	(200)	0.008	2	8	0.233	—	—	—

[1] The calculated ratio of $(b-c)/(a-c)$ differs from the value 0.25 because the addition of the rotational and tidal deformations is not linear unless $q \ll 1$ (Chandrasekhar 1969).

[2] Angle between the a-axis and the sub-planet direction.

[3] Data on Io are from Davies (1983).

[4] Data on Mimas and Enceladus are from Davies & Katayama (1983).

[5] The quoted mean density and radius of Miranda are nominal values.

[6] Radio measurements of the mass of Tethys by Voyager 2 yielded $(7.55\pm0.90)\times10^{23}$ g; the ratio of the libration amplitudes of Mimas and Tethys (the satellites are locked in a 2:1 inclination-type resonance) then provides a derived mass for Mimas of $(0.455\pm0.054)\times10^{23}$ g (Tyler *et al.* 1982). If the libration amplitudes and the libration period of Mimas alone are used (that is, the classical ground-based determination), then a significantly lower mass (0.385×10^{23} g) is obtained (Allen 1969).

Downloaded from rsta.royalsocietypublishing.org

communication 1984). Over and above these regular width variations, Nicholson & Matthews consider that there is evidence for irregular variations of magnitude of over 2 km. If these observations are substantiated, then I should consider that we have clear evidence for the existence of shepherding satellites. I should further expect these rings to show associated discrepancies in their precession rates (of both pericentre and node) of *upper* magnitude *ca.* 0.004 deg/day given, approximately, by (22).

A discrepancy $\delta\dot{\omega} \approx 0.005$ deg/day could be produced by satellites, for example, of mass ratios $m/M \approx 6 \times 10^{-10}$ or diameters *ca.* 40 km separated from the ring by *ca.* 300 km. (Note, the necessary masses increase as x^2.) Since the contributions to $\dot{\omega}$ of the J_4 term in (15) are about 0.02 deg/day, it follows that the contributions due to the shepherding satellites may have to be determined before J_4 is known with useful accuracy.

6. Shapes of satellites

If a satellite is rotating synchronously in a near-equatorial and near-circular orbit, and the tidal and rotational deformations are small ($q \ll 1$), then the total deformation of the satellite can be found by calculating these deformations separately and adding them linearly. The tidal potential U_t at some point (r, θ) within the satellite is given by

$$U_t = -(GM/a^3)\, r^2 P_2(\cos\theta), \tag{23}$$

where θ is the angle between r and the line joining the planet and satellite centres and $P_2(\cos\theta)$ is a Legendre polynomial. The rotational potential U_r at the same point is given by

$$U_r = \tfrac{1}{3}\Omega^2 r^2 P_2(\cos\phi), \tag{24}$$

where ϕ is the angle between r and the axis of rotation. From Kepler's third law we obtain

$$U_r = \tfrac{1}{3}(GM/a^3)\, r^2 P_2(\cos\phi). \tag{25}$$

As the deforming potentials are both second-degree solid harmonics, the theory that has been developed for rotational deformation can be applied directly to the tidal deformation. In particular, we can use the point-core model and the Darwin–Radau relation to place bounds on the total deformation (Dermott 1979*b*).

The differences between a, b and c, the principal radii of the triaxial ellipsoid that describes the satellite surface, are given by

$$(b-a)/(c-a) = \tfrac{1}{4}, \tag{26}$$

$$a - c = 5HqR. \tag{27}$$

For a homogeneous satellite in hydrostatic equilibrium H is unity. For all other internal density distributions H is bounded by

$$[\tfrac{1}{2} + \tfrac{25}{8}(1 - \tfrac{3}{2}C)^2]^{-1} \leqslant H \leqslant \tfrac{2}{5}[1 - \tfrac{3}{2}C]^{-1}, \tag{28}$$

where the lower limit is obtained from the Darwin–Radau relation and the upper limit from the point-core model (Dermott 1979*a*).

Values of a, b and c for Io, Mimas and Enceladus have been obtained by Davies (1983) and Davies & Katayama (1983) from Voyager images using an analytical triangulation programme:

Downloaded from rsta.royalsocietypublishing.org

see table 2 and figure 5. The results for Io are based on 10926 measurements of 650 control points on 203 Voyager 1 and 43 Voyager 2 images: 2018 linear simultaneous equations are solved in the analytical triangulation and the over-determination factor is 5.41. The results for Mimas and Enceladus are not so well determined (Davies & Katayama 1983).

The mean value of H for Mimas cannot be shown in figure 5, since values of $H < 0.4$ are physically impossible. The mean value of H for Io is possible but unrealistic. Values of C as low as 0.2 cannot be achieved unless the outer layers of a planetary body are gaseous: see §2. Most satellite models have $C \gtrsim 0.3$ and $H \gtrsim 0.7$. Consider, for example, the model satellites shown in figure 6. The model in figure 6*a* applies to Io and consists of a satellite of mean density

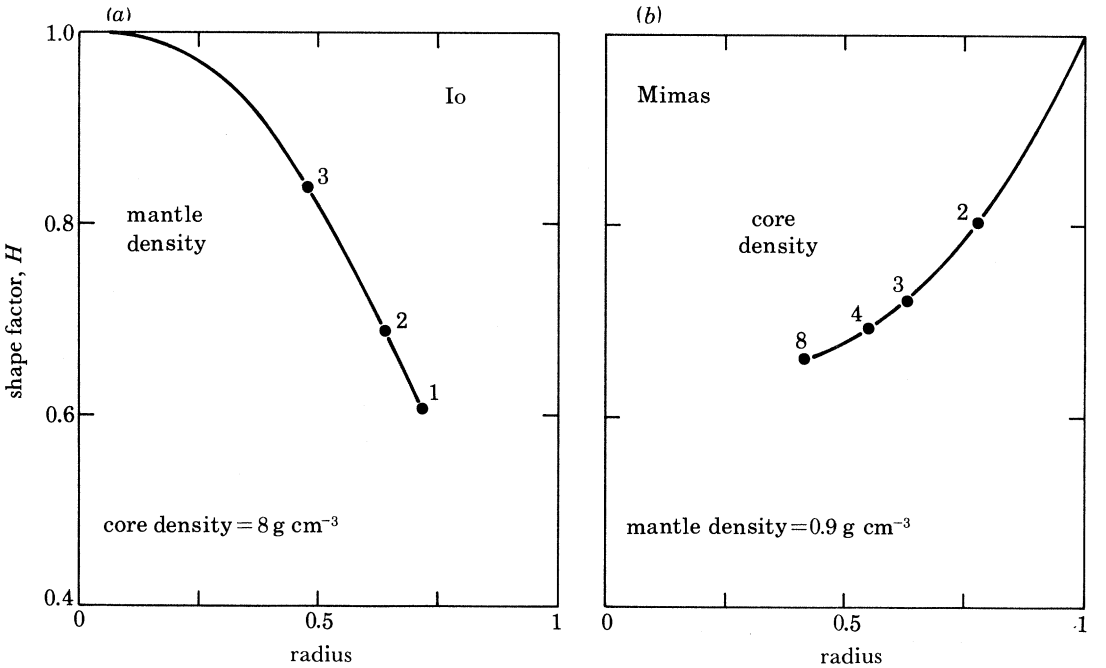

FIGURE 6. The shape factors H of (*a*) a satellite with the mean density of Io (3.56 g cm^{-3}), a uniform iron core of density 8 g cm^{-3} and a range of mantle densities and core radii, and (*b*) a satellite with the mean density of Mimas (1.42 g cm^{-3}), a uniform icy mantle of density 0.9 g cm^{-3} and a range of core densities and radii. In both cases, shape factors H much below 0.7 cannot be achieved with reasonable model interiors.

3.56 g cm^{-3} with a uniform iron core of density 8 g cm^{-3} and a uniform density mantle. Values of H are shown as a function of core radius: the numbers on the curve refer to the mantle density σ. Since, for the de-volatilized Io, we must expect $\sigma > 2$ g cm^{-3}, $H \gtrsim 0.7$. The model in figure 6*b* applies to Mimas and consists of a satellite of mean density 1.42 g cm^{-3} with a uniform icy mantle of density 0.9 g cm^{-3}. Values of H are again shown as a function of core radius, but the numbers on the curve now refer to the core density ρ. Since we must expect $\rho < 8$ g cm^{-3}, $H \gtrsim 0.66$.

If the mean density of Mimas is as high as 1.42 g cm^{-3} (the mass of Mimas obtained from the analysis of the Mimas–Tethys resonance by using ground-based observations of the libration period and the libration amplitude implies the much lower mean density of 1.16 ± 0.06 g cm^{-3}: see table 2), then the upper bound on the observed value of H is marginally consistent with a differentiated satellite with a large ($r \approx 0.5$), rocky-iron core and an icy

Downloaded from rsta.royalsocietypublishing.org

mantle. If the mantle has a density lower than that of water ice, or if the mean density of the satellite is more than 1.42 g cm^{-3}, then the observations of Davies *et al.* (1983) would be easier to account for.

If q is not very small, then the tidal and rotational deformations cannot be added linearly. The deformation of a homogeneous satellite in hydrostatic equilibrium has been calculated by Chandrasekhar (1969). His results can be described by

$$c/a = 1-5q-2.626q^2-174q^3, \tag{29}$$

$$b/a = 1-\tfrac{15}{4}q-12.7q^2-171q^3, \tag{30}$$

$$(b-c)/(a-c) = \tfrac{1}{4}(1-10q). \tag{31}$$

The calculated values listed in table 2 were obtained by using (29) and (30). For some of the inner satellites of the major planets, particularly Mimas, the deviations of the ratio $(b-c)/(a-c)$ from 0.25 are not negligible: see table 2. As q increases, b tends to c and the figure becomes more oblate and less triaxial. However, it would appear that these corrections for nonlinearity cannot account for the very small deformations of Mimas observed by Davies *et al.* (1983), even though these authors did assume that $(b-c)/(a-c) = 0.25$.

The spectacular volcanism of Io, the very high value of the observed heat output ($Q \gtrsim 1$ W m^{-2} (Pearl & Sinton 1982)) and the observation that the long-axis of the best-fit triaxial ellipsoid is significantly displaced from the sub-Jupiter direction (Davies 1983) suggest that the interior of Io is convecting and that the associated, horizontal variations of density may contribute to the observed figure (S. K. Runcorn, personal communication 1983).

The Navier–Stokes equation describing slow convection in a planetary interior, in which the forces arising from rotation may be neglected, is

$$\rho\nu\nabla^2\boldsymbol{v} = \nabla p + \boldsymbol{g}\alpha\rho T, \tag{32}$$

where ρ is the density, ν the kinematic viscosity, $\boldsymbol{v}$ the velocity, p the pressure, $\boldsymbol{g}$ the gravity, α the coefficient of volume expansion and T the temperature. Dimensional analysis of this equation gives

$$\rho\nu v/R^2 = g\Delta\rho_{\mathrm{h}}, \tag{33}$$

where $\Delta\rho_{\mathrm{h}}$ is a *horizontal* density difference. If we now make the approximations

$$\Delta\rho_{\mathrm{h}} = (h/R)\,\rho = \alpha\rho\Delta T_{\mathrm{h}} \tag{34}$$

and

$$Q = \rho C_p v \Delta T_{\mathrm{h}}, \tag{35}$$

where h is the height of the convective bulge, ΔT_{h} is a *horizontal* temperature difference and C_p is the specific heat, then we obtain

$$h = (\nu\alpha\kappa Q/gk)^{\frac{1}{2}}, \tag{36}$$

where κ $(= \kappa/\rho C_p)$ is the thermal diffusivity and k the thermal conductivity. Substituting $\alpha = 3\times10^{-5}$ K^{-1}, $\kappa = 10^{-6}$ m^2 s^{-1}, $g = 1.8$ m s^{-2} and $k = 4$W m^{-1} K^{-1} (Schubert *et al.* 1981) into this equation yields

$$h = 2\times10^{-6}\,\nu^{\frac{1}{2}}. \tag{37}$$

Downloaded from rsta.royalsocietypublishing.org

Thus, a substantial bulge of $h \approx 4$ km, for example, requires that Io has a kinematic viscosity of 4×10^{18} m^2 s^{-1}.

Tozer (1965) has argued that the viscosity of a convecting planetary interior is self-regulating and adjusts to a value consistent with the removal of the internally generated heat by convection and the minimization of the *vertical* (or radial) temperature difference ΔT_v. We estimate that

$$\nu = 0.0005\alpha g k^3 \Delta T_v^4 / \kappa Q^3 \tag{38}$$

(Schubert *et al.* 1981). From this and (36) we obtain

$$h = 0.02\alpha k \Delta T_v^2 / Q, \tag{39}$$

and, since ΔT_v cannot exceed *ca.* 1500 K, $h \approx 6$ m and can be neglected.

The upper bound on H for Io determined by Davies (1983) is consistent with that of a differentiated satellite with a large ($r \approx 0.5$) iron core; however, we cannot allow that the long axis is offset from the sub-Jupiter direction: perhaps it is merely a reflection of the uncertainty in H?

The comparatively smooth surface of Enceladus is a good indication that the mean surface of the satellite is close to hydrostatic equilibrium. A value of $a-c$ for Enceladus has been obtained by Davies & Katayama (1983), but the mean density of the satellite is uncertain and our formulae cannot be applied directly. (The satellite is involved in a resonance with Dione, but the amplitude of libration is very small and difficult to observe.) However, if a satellite is differentiated, which is probably the case for Enceladus, and has a deep mantle of known material (water ice, for example), then a determination of $a-c$ and R leads to useful estimates of the mean density, mass and moment of inertia. This statement applies if the core is of such a size and density that it can be sensibly replaced by a point mass. We would then have

$$H = \tfrac{2}{5}/[1 - \tfrac{3}{5}(\sigma/\langle\rho\rangle)] \tag{40}$$

and

$$\langle\rho\rangle = \tfrac{3}{5}\sigma + 3\Omega^2 R/2\pi G(a-c). \tag{41}$$

For example, if $a-c = 8$ km, $R = 251$ km (see table 2) and $\sigma = 0.9$ g cm^{-3}, then $\langle\rho\rangle = 1.2$ g cm^{-3}, $m = 7.9 \times 10^{22}$ g and $C = 0.30$. Here, I have assumed that the mantle has a uniform density but this is not essential to the argument. We only have to assume that the mantle has a known density distribution. The value of the mean density is consistent with that obtained from more direct estimates of the mass, but, to be useful, $a-c$ would need to be measured to within *ca.* 1 km.

This research was supported by NASA grant NAGW-392.

References

Alden, H. L. 1943 *Astr. J.* **50**, 110–111.
Allan, R. R. 1969 *Astr. J.* **74**, 497–506.
Allison, M. & Stone, P. H. 1983 Preprint. Saturn meteorology: a diagnostic assessment of thin layer configurations for the zonal flow, NASA, Goddard Space Flight Center. (In the press.)
Belton, M. J. S. & Terrile, R. J. 1984 *NASA spec. Publs.*
Belton, M. J. S., Wallace, L. & Howard, S. 1981 *Icarus* **46**, 263–274.
Brown, R. H., Cruikshank, D. P. & Tokunaga, A. T. 1981 *Icarus* **47**, 159–165.
Chandrasekhar, S. 1969 *Ellipsoidal figures of equilibrium.* New Haven: Yale University Press.
Darwin, G. H. 1899 *Mon. Not. R. astr. Soc.* **60**, 82–124.

PHILOSOPHICAL TRANSACTIONS OF THE ROYAL SOCIETY A MATHEMATICAL, PHYSICAL & ENGINEERING SCIENCES
PHILOSOPHICAL TRANSACTIONS OF THE ROYAL SOCIETY A MATHEMATICAL, PHYSICAL & ENGINEERING SCIENCES

Downloaded from rsta.royalsocietypublishing.org

Davies, M. E. 1983 '*Natural satellites*' *Meeting, Ithaca, New York.* (Contributed paper.)
Davies, M. E. & Katayama, F. Y. 1983 *Icarus* **53**, 332–340.
Dermott, S. F. 1979*a* *Icarus* **37**, 310–321.
Dermott, S. F. 1979*b* *Icarus* **37**, 575–586.
Dermott, S. F. 1981 *Nature, Lond.* **290**, 457–484.
Dermott, S. F. 1984 In *Planetary rings* (ed. A. Brahic & R. Greenberg). Tucson: University of Arizona Press. (In the press).
Desch, M. D. & Kaiser, M. L. 1981 *Geophys. Res. Lett.* **8**, 253–256.
Dunham, D. W. 1971 Ph.D. thesis, Yale University.
Elliot, J. L., French, R. G., Frogel, J. A., Elias, J. H., Mink, D. J. & Liller, W. 1981 *Astr. J.* **86**, 444–455.
Elliot, J. L. & Nicholson, P. D. 1984 In *Planetary rings* (ed. A. Brahic & R. Greenberg). Tucson: University of Arizona Press. (In the press.)
Franklin, F. A., Avis, C. C., Colombo, G. & Shapiro, I. I. 1980 *Astrophys. J.* **236**, 1031–1034.
Freedman, A., Tremaine, S. D. & Elliot, J. L. 1983 *Astr. J.* **88**, 1053–1059.
French, R. G. 1984 *NASA spec. Publs.* (In the press.)
French, R. G., Elliot, J. L. & Allen, D. A. 1982 *Nature, Lond.* **298**, 827–829.
French, R. G., Elliot, J. L., Dunham, E. W., Allen, D., Elias, J. H., Frogel, J. A. & Liller, W. 1983 *Icarus* **53**, 399–414.
French, R. G. & Taylor, G. E. 1981 *Icarus* **45**, 577–585.
Gehrels, T., Baker, L. R., Beshore, E., Blenman, C., Burke, J. J., Castillo, N. D., DaCosta, B., Degewij, J., Doose, L. R., Fountain, J. W., Gotobed, J., KenKnight, C. E., Kingston, R., McLaughlin, G., McMillan, R., Murphy, R., Smith, P. H., Stoll, C. P., Strickland, R. N., Tomasko, M. G., Wijesinghe, M. P., Coffeen, D. L. & Esposito, L. 1980 *Science, Wash.* **207**, 434–439.
Gill, J. R. & Gault, B. L. 1968 *Astr. J.* **73**, 595 (abstract).
Goldreich, P. & Tremaine, S. 1979 *Nature, Lond.* **277**, 97–99.
Goldreich, P. & Tremaine, S. 1982 *A. Rev. Astr. Astrophys.* **20**, 249–283.
Goody, R. M. 1982 In *Uranus and the outer planets* (ed. G. A. Hunt), pp. 143–153. Cambridge University Press.
Harris, A. W. 1984 *NASA spec. Publs* (In the press.)
Hubbard, W. B. 1982 *Icarus* **52**, 509–515.
Hubbard, W. B. 1984 *NASA spec. Publs* (In the press.)
Ingersoll, A. P. & Pollard, D. 1982 *Icarus* **52**, 62–80.
Jeffreys, H. 1970 *The Earth.* Cambridge University Press.
Julian, W. H. & Toomre, A. 1966 *Astrophys. J.* **146**, 810–832.
Kovalevsky, J. & Link, F. 1969 *Astron. Astrophys.* **2**, 398–412.
Lindal, G. F., Wood, G. E., Levy, G. S., Anderson, J. D., Sweetham, D. N., Hotz, H. B., Buckles, B. J., Holmes, D. P., Doms, P. E., Eshleman, V. K., Tyler, G. L. & Croft, T. A. 1981 *J. geophys. Res.* **86**, 8721–8727.
Null, G. W. 1976 *Astr. J.* **81**, 1153–1161.
Null, G. W., Lau, E. L., Biller, E. D. & Anderson, J. D. 1981 *Astr. J.* **86**, 456–468.
O'Meara, S. J. 1984 I.A.U. Circ. no. 3912, 1 February.
Pearl, J. C. & Sinton, W. M. 1982 In *Satellites of Jupiter* (ed. D. Morrison), pp. 724–755. Tucson: University of Arizona Press.
Schubert, G., Stevenson, D. J. & Ellsworth, K. 1981 *Icarus* **47**, 46–49.
Slavsky, D. & Smith, H. J. 1978 *Astrophys. J.* **226**, L49–L52.
Smith, B. A., Reitsema, H. J. & Larson, S. M. 1979 *Bull. Am. astr. Assoc.* **11**, 570.
Smoluchowski, R. 1976 In *Jupiter* (ed. T. Gehrels), pp. 3–21. Tucson: University of Arizona Press.
Terrile, R. J. & Smith, B. A. 1983 *Bull. Am. Astr. Assoc.* **15**, 858.
Terrile, R. J., Smith, B. A. & Avis, C. C. 1984 (In preparation.)
Tozer, D. C. 1965 *Phil. Trans. R. Soc. Lond.* A **258**, 252–271.
Tyler, G. L., Eshleman, V. R., Anderson, J. D., Levy, G. S., Lindal, G. F., Wood, G. E. & Croft, T. A. 1982 *Science, Wash.* **215**, 553–558.

Discussion

A. H. Jupp (*University of Liverpool, Liverpool, U.K.*). Dr Dermott's equation for the secular rate of change of the apse longitude, from which he computes J_4, puzzles me. The approximate values he gives for J_2 and J_4 are such that $J_2^2 = O(J_4)$. It would seem to be the case, therefore, that the equation referred to should contain the second-order contribution from J_2^2 in addition to the linear terms in J_2 and J_4 which he includes. The consequences of this correction would probably change his value of J_4 and also the gradients of some of the graphs he has shown us.

PHILOSOPHICAL TRANSACTIONS OF THE ROYAL SOCIETY A MATHEMATICAL, PHYSICAL & ENGINEERING SCIENCES
PHILOSOPHICAL TRANSACTIONS OF THE ROYAL SOCIETY A MATHEMATICAL, PHYSICAL & ENGINEERING SCIENCES

Downloaded from rsta.royalsocietypublishing.org

S. F. Dermott. The expression which I give for the secular rate of change of the apse longitude, $\dot{\tilde{\omega}}$, does not contain a J_2^2 term but it is correct. The differences between the many different expressions for $\dot{\tilde{\omega}}$ that appear in the literature have been reconciled by Greenberg (1981). The particles in the rings of Uranus precess as a whole, and at the level at which the J_2^2 and the J_4 terms are important one must be careful to distinguish between the geometrical parameters describing the elliptical ring and the osculating orbital elements of the particles moving in the ring. In equations (15) and (16) a is the observed (not the osculating Keplerian) semimajor axis of the ring.

Reference

Greenberg, R. J. 1981 *Astr. J.* **86**, 912–914.

PHILOSOPHICAL TRANSACTIONS OF THE ROYAL SOCIETY A MATHEMATICAL, PHYSICAL & ENGINEERING SCIENCES

PHILOSOPHICAL TRANSACTIONS OF THE ROYAL SOCIETY A MATHEMATICAL, PHYSICAL & ENGINEERING SCIENCES